Eur. Phys. J. D (2014)
DOI: 10.1140/epjd/e2013-40743-7

THE EUROPEAN PHYSICAL JOURNAL D

Regular Article

The two-particle two-slit experiment

Pedro Sancho[a]

Centro de Láseres Pulsados CLPU, Parque Científico, 37085 Villamayor, Salamanca, Spain

Received 25 November 2013
Published online (Inserted Later) – © EDP Sciences, Società Italiana di Fisica, Springer-Verlag 2014

Abstract. Identical two-particle interferometry provides a scenario where interference and exchange effects manifest at once. We present a detailed calculation of the detection patterns in the two-particle two-slit experiment by extending Feynman's Gaussian slit approach to multi-mode states. We show the existence of two regimes depending on the mode distributions. In one of them we find a novel behavior for bosons, with detection patterns almost equal to those of distinguishable particles although the overlapping is large. As a byproduct of our analysis we conclude that the interaction at the diffraction grating is an efficient method to increase the initial overlapping. We propose a scheme, within the reach of present day technology, to experimentally verify our results.

1 Introduction

Multi-photon interference, specially two-photon one, has been extensively studied in Quantum Optics after the seminal Hong-Ou-Mandel work (HOM) [1,2]. More recently, similar ideas have been presented for identical massive particles [3–9]. Identical multi-particle interference is interesting because two fundamental principles of quantum theory, interference and (anti)symmetrization of the states of identical particles, act simultaneously in the system. Interference and exchange effects can be observed at once.

In previous proposals of massive multi-particle interferometry no detailed evaluation of the detection patterns has been presented. Such an evaluation is necessary for comparison with the results of any potential experimental test. For instance, in reference [7] a calculation of the two-particle one-slit patterns has been carried out, but with an oversimplified state. It is necessary to consider more realistic states. We do it here for the two-slit arrangement.

The two-slit experiment is the archetypical example of quantum interference. It has been used on countless occasions to illustrate the wave properties of quantum systems. However, the massive two-particle counterpart of the arrangement (with a detailed evaluation of the expected patterns) has not been discussed in the literature. As it is well known, the exact evaluation of the wave function of a particle passing through a slit demands the use of Fresnel's functions, complicating the understanding of the problem. In order to carry out the discussion in mathematical terms as simple as possible we resort to Feynman's Gaussian slit approximation, used in the path integrals formalism [10]. Moreover, to make the evaluation more realistic, we shall consider particles in multi-mode states instead of the single-mode one presented in reference [10].

[a] e-mail: psanchos@aemet.es

In the above approximation we can determine the two-particle detection patterns, which show the existence of two regimes. For similar mode distributions of the two particles (in a sense discussed quantitatively later) the patterns of distinguishable particles and bosons are almost equal and indistinguishable from the experimental point of view. In contrast, fermions patterns are clearly different. When the mode distributions are not similar we have another regime where the three types of patterns are easily distinguishable.

As we shall see later, in the first regime we have in general a large overlapping. Then we should expect an important contribution of the exchange effects and, as in the HOM experiment, a clearly differentiated behavior of bosons and distinguishable particles. The unexpected behavior found in that regime can be explained by the simultaneous contribution of the large final overlapping to the form of the two-particle wave function and its normalization, two factors that cancel each other out. As a byproduct of the analysis we shall show that the interaction at the diffraction grating increases the initial overlapping of the particles.

In the final part of the paper we propose a scheme for the experimental verification of two-atom two-slit interferometry. The source of a single particle diffraction arrangement is replaced by one of (anti)symmetrized two-particle states using techniques of atom lasers [11], making possible the comparison of the two-particle detection patterns of bosons and fermions with these of distinguishable particles.

2 General expressions for two-particle systems

Our arrangement is a standard two-slit interference device, but with the source emitting pairs of particles.

The particles can be distinguishable or identical. After the slits we place detectors that determine the joint patterns by counting arrivals on coincidence. We denote the two slits by A and B. The two particles are in the states $\psi(x)$ and $\phi(y)$, with x and y their coordinates. If we consider detections in a plane parallel to the slits we can reduce the problem to an one-dimensional one, as we do here. The first wave function can be expressed as:

$$\psi(x) = N_\psi(\psi_A(x) + \psi_B(x)) \tag{1}$$

with N_ψ the normalization coefficient, deduced from $\int dx|\psi(x)|^2 = 1$. A similar expression holds for ϕ.

If the two particles are distinguishable the state of the two-particle system is a product one:

$$\Phi(x, y) = \psi(x)\phi(y). \tag{2}$$

Note that this state is already normalized, $\int\int dxdy|\Phi(x, y)|^2 = 1$, because of the previous normalization of ψ and ϕ.

When the two particles are identical the joint state is:

$$\Psi(x, y) = N_\Psi \left(\psi(x)\phi(y) \pm \psi(y)\phi(x)\right). \tag{3}$$

In the double sign expression $\pm$ the upper one refers to bosons and the lower one to fermions. The normalization factor is:

$$N_\Psi = \frac{1}{\left(2 \pm 2|\left\langle\psi|\phi\right\rangle|^2\right)^{1/2}} \tag{4}$$

where, for the matter of simplicity, we have used the ket notation $\langle\psi|\phi\rangle = \int dx\psi^*(x)\phi(x)$.

From these expressions we can derive the probability densities of joint detection. In the distinguishable case, in order to obtain a more compact presentation (in the comparison with the identical case, where there is an interchange of the coordinates x and y) it is natural to present the results in a more symmetric way. In equation (2) the particles in states ψ and ϕ are labeled by x and y. Similarly, we could denote them by y and x ($\psi(y)$ and $\phi(x)$). Then the symmetric presentation of the probability density for distinguishable particles is:

$$P_{dis}(x, y) = \frac{1}{2}|\Phi(x, y)|^2 + \frac{1}{2}|\Phi(y, x)|^2. \tag{5}$$

For identical particles the density probability is $P(x, y) = |\Psi(x, y)|^2$. After a simple calculation we have:

$$P(x, y) = 2|N_\Psi|^2 P_{dis}(x, y) \pm 2|N_\Psi|^2 \times \sum_{i_1,i_2,i_3,i_4}^{A,B} \mathrm{Re}\left(\psi^*_{i_1}(x)\phi^*_{i_2}(y)\psi_{i_3}(y)\phi_{i_4}(x)\right). \tag{6}$$

In the above sum the indexes $i_1, i_2, \ldots$ run over the two alternatives available for each particle, A and B.

The probability density is given by the sum of two terms, the direct and exchange ones. Note that there are sixteen exchange terms associated with the eight alternatives present in the problem (the first alternative is the particle in state ψ going through slit A and the particle in state ϕ also passing through A, ...).

3 Feynman's Gaussian slit approximation

Our next step is to derive the wave functions of the particles after the slits, for instance, ψ_A. The source is placed at point $x = 0$ and the middle point of the slit (with a width $2b$) at x_0. The particle is initially in a multi-mode state described by the distribution [12]

$$f(k) = \frac{(4\pi)^{1/4}}{\sigma^{1/2}} \exp\left(-k^2/2\sigma^2\right). \tag{7}$$

This is a Gaussian function with mean value $k_0 = 0$. The wave function in the position space is given by:

$$\psi_A(x, t) = (2\pi)^{-1} \int dk f(k) \exp\left(i\left(kx - k^2\hbar t/2m\right)\right) = C(t) \exp\left(\frac{-\sigma^2x^2 + i\hbar\sigma^4x^2t/m}{\mu(t)}\right) \tag{8}$$

with

$$C(t) = \pi^{-1/4}\left(\frac{1}{\sigma} + \frac{i\hbar\sigma t}{m}\right)^{-1/2}; \mu(t) = 2\left(1 + \frac{\hbar^2\sigma^4t^2}{m^2}\right). \tag{9}$$

Equation (8) differs from equation (17) in reference [12] by the absence of a factor 2 in the second term of the numerator of the exponential.

The particle evolves free up to the slit. After the slit the wave function can be expressed using the path integral formalism [10]

$$\psi_A(x, t) = \int_{slit} dx_s K(x, t; x_s, t_s)\psi_A(x_s, t_s), \tag{10}$$

where the subscript s refers to the coordinates of the slit (x_s) and the time when the particle reaches it (t_s). The integration is over all the extension of the slit (for the rest of the paper, when no explicit range of integration is included we refer to $(-\infty, \infty)$). K denotes the kernel of the problem which is well known to be [10]

$$K(x, t; x_s, t_s) = \left(\frac{m}{2\pi i\hbar(t - t_s)}\right)^{1/2} \exp\left(\frac{im(x - x_s)^2}{2\hbar(t - t_s)}\right). \tag{11}$$

As signalled in Section 1 the above integral leads to Fresnel's functions, making impossible to deal analytically with the problem. Thus, to present a more intuitive physical picture of the problem we avoid, following Feynman, the use of the Fresnel functions by introducing the Gaussian slit approximation. In this approach the integration is extended to all the axis, but with a weight function $\exp(-(x_s - x_0)^2/2b^2)$ that reduces the relevant values of the integrand to the proximity of the slit. Explicitly, we have:

$$\psi_A(x, t) = \int dx_s e^{-(x_s - x_0)^2/2b^2} K(x, t; x_s, t_s)\psi_A(x_s, t_s). \tag{12}$$

After a simple calculation we obtain:

$$\psi_A(x, t) = \mathcal{C}e^{imx^2/2\hbar(t - t_s)}e^{-(\alpha - i\beta)x^2}e^{-(\delta + i\gamma)x} \tag{13}$$

with

$$\mathcal{C} = C(t_s)\left(\frac{m}{2i\hbar(t-t_s)(D+iF)}\right)^{1/2} \times e^{-x_0^2/2b^2} e^{G^2(D-iF)/4\left(D^2+F^2\right)} \quad (14)$$

$$\alpha = \frac{DH^2}{4\left(D^2+F^2\right)}; \quad \beta = \frac{FH^2}{4(D^2+F^2)};$$

$$\gamma = \frac{DGH}{2\left(D^2+F^2\right)}; \quad \delta = \frac{GHF}{2(D^2+F^2)} \quad (15)$$

and

$$D = \frac{1}{2b^2} + \frac{\sigma^2}{\mu}; \quad F = -\frac{\hbar\sigma^4 t_s}{m\mu} - \frac{m}{2\hbar(t-t_s)};$$

$$G = \frac{x_0}{b^2}; \quad H = \frac{m}{\hbar(t-t_s)}. \quad (16)$$

4 Two-particle probability densities

The expressions for the other wave functions are similar to equation (13):

$$\psi_B(x,t) = \mathcal{C} e^{imx^2/2\hbar(t-t_s)} e^{-(\alpha-i\beta)x^2} e^{(\delta+i\gamma)x} \quad (17)$$

$$\phi_A(x,t) = \overline{\mathcal{C}} e^{imx^2/2\hbar(t-t_s)} e^{-\left(\overline{\alpha}-i\overline{\beta}\right)x^2} e^{-\left(\overline{\delta}+i\overline{\gamma}\right)x} \quad (18)$$

and

$$\phi_B(x,t) = \overline{\mathcal{C}} e^{imx^2/2\hbar(t-t_s)} e^{-\left(\overline{\alpha}-i\overline{\beta}\right)x^2} e^{\left(\overline{\delta}+i\overline{\gamma}\right)x}. \quad (19)$$

All the coefficients of the particle in state ϕ are denoted by an overline. The width of the mode distribution in this case is $\overline{\sigma}$, giving rise to different $\overline{D}$ and $\overline{F}$ and, consequently, different $\overline{\mathcal{C}}$, $\overline{\alpha}, \ldots$ The different widths of the initial multi-mode states is the parameter we use to control the initial overlapping of the two particles. On the other hand, H is equal in all the cases and G changes its sign for the slit B, leading to the modifications $\gamma \to -\gamma, \ldots$, $\overline{\delta} \to -\overline{\delta}$. Finally, $\exp(imx^2/2\hbar(t-t_s))$ is equal for the four terms and will cancel in the calculation of probability densities.

Using these expressions we can derive the normalization coefficients and the detection patterns. The normalization coefficients are:

$$N_\psi = \frac{1}{|\mathcal{C}|}\left(\frac{\alpha}{2\pi}\right)^{1/4}\left(e^{\delta^2/2\alpha} + e^{-\gamma^2/2\alpha}\right)^{-1/2} \quad (20)$$

and a similar expression for N_ϕ with obvious modifications. N_Ψ is given by equation (4), where $|\langle\psi|\phi\rangle|^2$ can be calculated from

$$\frac{1}{\mathcal{C}^*\overline{\mathcal{C}} N_\psi N_\phi}\left(\frac{(\alpha+\overline{\alpha}) + i\left(\beta-\overline{\beta}\right)}{\pi}\right)^{1/2}\langle\psi|\phi\rangle$$
$$= \exp\left(\frac{\left(\left(\delta+\overline{\delta}\right) - i\left(\gamma-\overline{\gamma}\right)\right)^2}{4\left((\alpha+\overline{\alpha}) + i\left(\beta-\overline{\beta}\right)\right)}\right)$$
$$+ \exp\left(\frac{\left(\left(\delta-\overline{\delta}\right) - i\left(\gamma+\overline{\gamma}\right)\right)^2}{4\left((\alpha+\overline{\alpha}) + i\left(\beta-\overline{\beta}\right)\right)}\right)$$
$$+ \exp\left(\frac{\left(\left(\overline{\delta}-\delta\right) + i\left(\gamma+\overline{\gamma}\right)\right)^2}{4\left((\alpha+\overline{\alpha}) + i\left(\beta-\overline{\beta}\right)\right)}\right)$$
$$+ \exp\left(\frac{\left(-\left(\delta+\overline{\delta}\right) + i\left(\gamma-\overline{\gamma}\right)\right)^2}{4\left((\alpha+\overline{\alpha}) + i\left(\beta-\overline{\beta}\right)\right)}\right). \quad (21)$$

Finally, we evaluate the detection patterns. From the experimental point of view they are measured by placing a detector at a fixed position x and by moving another detector along the y-axis. We choose $x = 0$ and obtain

$$P_{dis}(0,y)/\left(|\mathcal{C}|^2\left|\overline{\mathcal{C}}\right|^2 N_\psi^2 N_\phi^2\right) = 2e^{-2\alpha y^2}\left(e^{-2\delta y} + e^{2\delta y}\right)$$
$$+ 2e^{-2\overline{\alpha}y^2}\left(e^{-2\overline{\delta}y} + e^{2\overline{\delta}y}\right)$$
$$+ 4e^{-2\alpha y^2}\cos(2\gamma y)$$
$$+ 4e^{-2\overline{\alpha}y^2}\cos\left(2\overline{\gamma}y\right) \quad (22)$$

and

$$\left(e^{(\alpha+\overline{\alpha})y^2}/\left|\mathcal{C}\right|^2\left|\overline{\mathcal{C}}\right|^2 N_\psi^2 N_\phi^2\right)$$
$$\times \sum_{i_1,i_2,i_3,i_4}^{A,B} \mathrm{Re}\left(\psi_{i_1}^*(0)\phi_{i_2}^*(y)\psi_{i_3}(y)\phi_{i_4}(0)\right)$$
$$= 4e^{-\left(\delta+\overline{\delta}\right)y}\cos\left(\left(\beta-\overline{\beta}\right)y^2 + \left(\overline{\gamma}-\gamma\right)y\right)$$
$$+ 4e^{\left(\delta+\overline{\delta}\right)y}\cos\left(\left(\beta-\overline{\beta}\right)y^2 - \left(\overline{\gamma}-\gamma\right)y\right)$$
$$+ 4e^{\left(\delta-\overline{\delta}\right)y}\cos\left(\left(\beta-\overline{\beta}\right)y^2 + \left(\overline{\gamma}+\gamma\right)y\right)$$
$$+ 4e^{-\left(\delta-\overline{\delta}\right)y}\cos\left(\left(\beta-\overline{\beta}\right)y^2 - \left(\overline{\gamma}+\gamma\right)y\right). \quad (23)$$

5 Results

Using the above equations we can graphically represent the behavior of the joint detection probability densities. First of all, we choose numerical values for the parameters of the problem. Typical values of the slit size and separation between the slits are of the order of 1 μm. Usual separations between the source and diffraction grating are close to half a meter, and velocities perpendicular to the plane of the diffraction grating vary in a wide range (10^2 to 10^7 $\mathrm{m\,s^{-1}}$). For instance, for atoms typical values are around 3×10^3 $\mathrm{m\,s^{-1}}$. Then we can take for the time of fly 10^{-4} to 10^{-5} s and $\hbar t_s/m \approx 1$ $\mu\mathrm{m}^2$ (similarly,

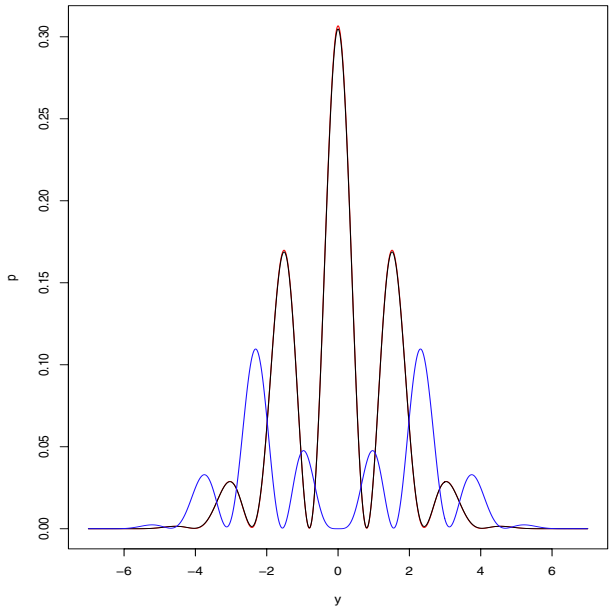

Fig. 1. Probability density of simultaneous detection (in $\mu\mathrm{m}^{-2}$) versus position of the moving detector y (in μm) for the values signaled in the text. The black, red and blue curves correspond respectively to distinguishable particles, fermions and bosons.

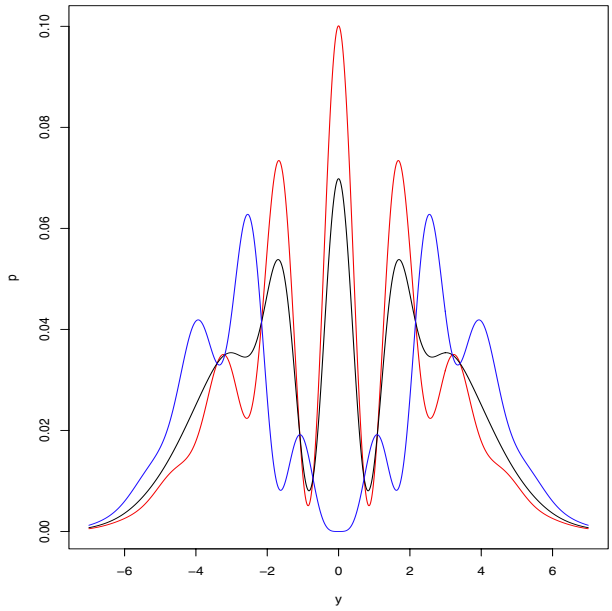

Fig. 2. The same as Figure 1 but for $\overline{\sigma} = 4\ \mu\mathrm{m}^{-1}$.

for $\hbar(t - t_s)/m$). The dispersion of the initial wavepacket ($\sigma \approx \Delta k$) in the axis parallel to the diffraction grating can be expressed in terms of the dispersion of the particle velocity in that direction, $\sigma \approx m\Delta v/\hbar$. Taking into account the perpendicular velocity and source-grating separation we must have $\Delta v \approx 10^{-1}\ \mathrm{m\,s}^{-1}$ (the probability of reaching the slits for particles with much larger parallel velocities is negligible). This corresponds to $\sigma \approx 1\ \mu\mathrm{m}^{-1}$.

We choose for our representation the values $b = 0.1\ \mu$m, $x_0 = 0.4\ \mu$m. $\hbar t_s/m = \hbar(t-t_s)/m = 0.2\ \mu\mathrm{m}^2$, $\sigma = 1\ \mu\mathrm{m}^{-1}$ and $\overline{\sigma} = 2\ \mu\mathrm{m}^{-1}$. The most relevant fact (see Fig. 1) is that the curves for bosons and distinguishable particles are almost equal. In contrast, the behavior of fermions is clearly different.

Next, we represent (see Fig. 2) the detection patterns with the same parameters of Figure 1 but with a larger spread of the initial wavepacket, $\overline{\sigma} = 4\ \mu\mathrm{m}^{-1}$. Now, the situation drastically changes with patterns clearly different for bosons and distinguishable particles, and again for fermions.

The trend observed in the two above figures is general. For all the $\overline{\sigma}$ smaller than approximately $2.5\ \mu\mathrm{m}^{-1}$ the curves of distinguishable particles and bosons are almost equal. For other values of the parameters b, x_0, ... the critical value of $\overline{\sigma}$ changes, but the behavior is the same. We can easily understand this property in terms of the final overlapping between the particles after the diffraction grating. The overlapping is measured in terms of $|\langle\psi|\phi\rangle|^2$, which reaches the maximum value 1 for full overlapping ($\phi = \psi$) and decreases to 0 for orthogonal wave functions with null overlapping. We represent it in Figure 3.

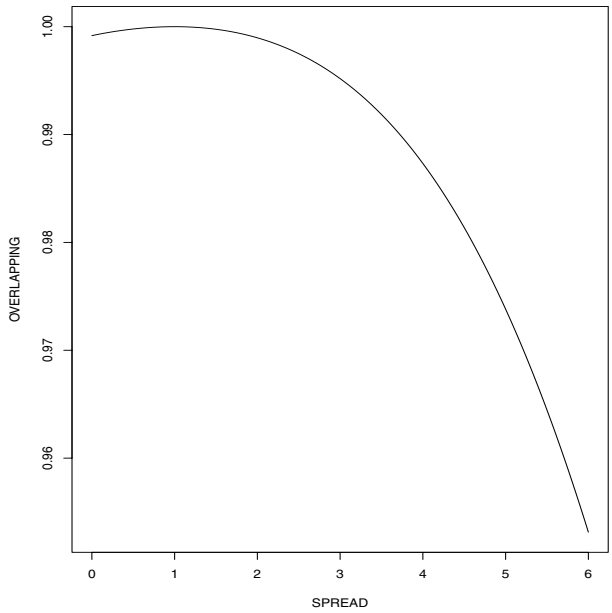

Fig. 3. Dimensionless overlapping after the diffraction grating versus initial spread of one of the particles $\overline{\sigma}$ (in $\mu\mathrm{m}^{-1}$, with σ fixed to $1\ \mu\mathrm{m}^{-1}$).

We see that for approximately $\overline{\sigma} < 2.5\ \mu\mathrm{m}^{-1}$ the final overlapping is very close to unity. For bosons the full wave function can be expressed as $\Psi_B(x,y) \approx 2\psi(x)\psi(y)/\sqrt{2+2} \approx \psi(x)\psi(y)$ (because $|\langle\psi(x)|\phi(x)\rangle|^2 \approx 1$ implies $\psi(x) \approx \phi(x)$). Then the two-particle wave function for bosons is almost equal to that of distinguishable particles, a product state, and we must expect almost equal detection patterns in both cases. For fermions the situation is different. In the limit of complete overlapping we have, $\Psi_F(x,y) \to (1-1)\psi(x)\psi(y)/\sqrt{2-2}$, an undefined expression of the type $0/0$ reflecting Pauli's

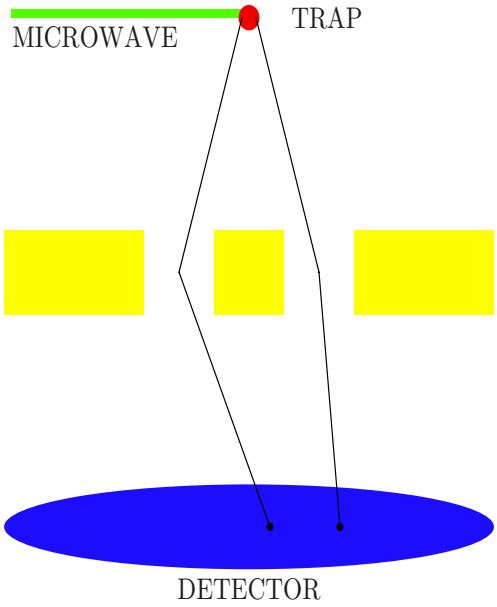

Fig. 4. The continuous microwave beam ejects atoms from the trap at a slow rate.

exclusion principle. However, for values very close to unity of the overlapping we have the quotient of two very small numbers but that is well defined and, as shown by Figure 1, different from the distinguishable case.

As a byproduct of the above analysis we obtain a potentially interesting application. We compare the initial and final overlapping, that is, prior and subsequent to the interaction with the diffraction grating. The initial overlapping is given by $2\sigma\overline{\sigma}/(\sigma^2+\overline{\sigma}^2)$. We have that the initial overlapping for $\overline{\sigma} = 0.1, 0.5, 2$ and $4\ \mu\mathrm{m}^{-1}$ (and $\sigma = 1\ \mu\mathrm{m}^{-1}$) is $0.2, 0.48, 0.47$ and 0.12, whereas the final overlapping is 0.99 for the three first cases and 0.39 for the fourth one. The diffraction grating acts as an efficient mechanism if we use it as a device to increase the overlapping of the pair of particles.

6 Experimental tests

We briefly propose in this section a scheme able to test the two-atom two-slit patterns with present day technology. We shall mainly resort to the techniques of atom laser generation. For the sake of concreteness we shall focus on the arrangement described in reference [11], which is specially well suited for our purposes.

Our starting point is the two-particle source. It consists of a trap containing a large number of atoms (see Fig. 4). We extract atoms from the trap in a controlled way. This can be done using a microwave beam. For instance, in reference [11] the ^{87}Rb atoms in the magnetic trap are in the hyperfine ground state $|F=1, m_F=-1\rangle$. The microwave spin-flips some atoms into the state $|F=2, m_F=0\rangle$. These atoms do not feel the trapping interaction and escape. Then the atoms fall by gravity and reach the diffraction grating. The joint patterns are subsequently measured by atom detection within a temporal coincidence window.

The critical points in the scheme are, (i) to make the escaping rate small enough in order to have small probabilities of a large number of released atoms in the time interval defined by the coincidence window; and (ii) to guarantee that the atoms detected in that window have a non-negligible overlapping giving rise to exchange effects. The two conditions can be fulfilled by the extraction method in reference [11]. With respect to (ii) it must be remarked that the microwave beam cannot be monochromatic because this would lead to an atom laser without bunching. Instead, we must use a broadband beam with noise (a pseudo-thermal beam), in which bunching effects are present [11]. The presence of these effects certifies the existence of overlapping between the atoms. Moreover, varying the chromatic composition of the beam we could control the overlapping degree. On the other hand, concerning (i), the counting statistics (for a detection time interval of 1.5 ms and a flux close to 5 atoms per ms) in the pseudo-thermal case agrees with a Bose distribution of mean value 1.99. The probability of time intervals with five or more detections is small, but the probability of one or three detections during a single interval is comparable to that of two events. Then we must introduce a postselection routine to eliminate the cases with one and three or more detections in the coincidence window (note, as we shall see later, that the coincidence window is much shorter than the time interval used to determine the counting statistics). This routine also eliminates the cases where two atoms are released from the trap during the coincidence window but one of them is absorbed by the wall delimiting the slits.

With respect to the detectors, we suggest to consider the same type used in reference [13], which is space- and time-sensitive. This way we can resolve the point and time of arrival of each particle. The coincidence window can be close to the values 25 μs [13] or 50 μs [11] used as time bin sizes to construct the histograms in these references.

The above discussion has been carried out with bosons. The extension to fermions follows the same lines. Instead of the BEC of [11] we must consider a trap containing a degenerate Fermi gas. Using the adequate output coupling we can extract fermions from the trap in a controlled way.

7 Discussion

We have explicitly evaluated the joint detection patterns of the two-particle two-slit arrangement. The calculations are based on the extension of Feynman's Gaussian slit approximation to multi-mode states. This approximation allows for an analytical approach to the problem.

The detection patterns of bosons, fermions and distinguishable particles are clearly different in the regime of distant mode distributions (in the space of distribution functions). When these mode distributions are close the behavior of bosons and distinguishable particles is almost identical due to the large final overlapping.

The behavior of bosons in the second case is counterintuitive. With large overlapping we in general expect the exchange effects to be also large and the detection patterns of identical and distinguishable particles to differ. This is so in the HOM arrangement. In particular, when the photons overlapping is close to unity (and the reflection and transmission coefficients are equal) we can observe the famous HOM dip, with no pair of photons leaving the beam splitter in different arms. This pattern contrasts with that of no-overlapping photons where the probability for one photon emerging in each output arm is 1/2 [2]. The difference between our system and the HOM one lies in the form of the final states. In our case the almost unity final overlapping leads to almost equal final wave functions and the approximate form $2\psi(x)\psi(y)$ for the numerator of $\Psi(x,y)$. The coefficient 2, for very large overlapping, cancels with the denominator, $(2+2|\langle\psi|\phi\rangle|^2)^{1/2} \approx 2$. Ψ approximately reduces to a product state characteristic of distinguishable particles. In contrast, in the HOM case the two-photon state after the beam splitter only adopts the form corresponding to photons that reflect and transmit independently (the form we expect for particles that, in the absence of exchange interactions, evolve independently) when the overlapping is null: for large overlapping there is not a cancelation effect of the type present in our arrangement. Up to our knowledge, this counterintuitive type of behavior of the bosons has not been previously described in the literature.

The differentiated behavior of the three types of particles shows the simultaneous presence of interference and exchange effects. In particular, we have a manifestation of exchange interactions potentially verifiable and different from (anti)bunching. This is interesting because (anti)bunching tests have dominated the experimental arena in the search of effects associated with the statistics of massive particles during the last years (see [13] and references therein).

We have also shown that interference at the diffraction grating is an efficient method to generate large degrees of overlapping. This point could be of interest in the preparation of (anti)symmetrized states.

A scheme to experimentally test the results of this paper in atomic systems has been presented. It is based on existent techniques and then seems to be a realistic proposal. It can be easily extended to other types of two-particle interferences and could, with minor modifications, be used to test the arrangements discussed in references [3,7,8]. In the same line of this proposal we could also test simultaneously interference and exchange effects in many-particle systems instead of only two-particle ones. By similitude with the experiment in reference [13] we can turn off the trapping potential, releasing all the atoms at the same time. After interaction with a diffraction grating and detection, the observed correlation functions would contain information on the interference device parameters and particle statistics. The many-particle experiment would be much less demanding than the two-particle one.

I acknowledge support from Spanish Ministerio de Ciencia e Innovación through the research project FIS2009-09522.

References

1. C.K. Hong, Z.Y. Ou, L. Mandel, Phys. Rev. Lett. **59**, 2044 (1987)
2. R. Loudon, *The Quantum Theory of Light* (Oxford University Press, Oxford, 2000)
3. M.P. Silverman, *More than one Mistery: Explorations in Quantum Interference* (Springer-Verlag, New York, 1995)
4. S. Bose, D. Home, Phys. Rev. Lett. **88**, 050401 (2002)
5. Y.L. Lim, A. Beige, New J. Phys. **7**, 155 (2005)
6. V. Giovannetti, Laser Phys. **16**, 1406 (2006)
7. P. Sancho, J. Phys. B **43**, 066504 (2010)
8. P. Sancho, Phys. Rev. A **82**, 033814 (2010)
9. P. Sancho, J. Phys. B **44**, 145002 (2011)
10. R.P. Feynman, A.R. Hibbs, *Quantum Mechanics and Path Integrals* (McGraw-Hill Book Company, New York, 1965)
11. A. Öttl, S. Ritter, M. Köhl, T. Esslinger, Phys. Rev. Lett. **95**, 090404 (2005)
12. C.S. Adams, M. Siegel, J. Mlynek, Phys. Rep. **240**, 143 (1994)
13. T. Jeltes et al., Nature **445**, 402 (2007)